

University of Groningen

Computer Simulation Study of Bipolaron Formation

Raedt, H. De; Lagendijk, A.

Published in:
Zeitschrift für Physik. B: Condensed Matter

DOI:
[10.1007/BF01308398](https://doi.org/10.1007/BF01308398)

IMPORTANT NOTE: You are advised to consult the publisher's version (publisher's PDF) if you wish to cite from it. Please check the document version below.

Document Version
Publisher's PDF, also known as Version of record

Publication date:
1986

[Link to publication in University of Groningen/UMCG research database](#)

Citation for published version (APA):

Raedt, H. D., & Lagendijk, A. (1986). Computer Simulation Study of Bipolaron Formation. *Zeitschrift für Physik. B: Condensed Matter*, 65(1). <https://doi.org/10.1007/BF01308398>

Copyright

Other than for strictly personal use, it is not permitted to download or to forward/distribute the text or part of it without the consent of the author(s) and/or copyright holder(s), unless the work is under an open content license (like Creative Commons).

The publication may also be distributed here under the terms of Article 25fa of the Dutch Copyright Act, indicated by the "Taverne" license. More information can be found on the University of Groningen website: <https://www.rug.nl/library/open-access/self-archiving-pure/taverne-amendment>.

Take-down policy

If you believe that this document breaches copyright please contact us providing details, and we will remove access to the work immediately and investigate your claim.

Downloaded from the University of Groningen/UMCG research database (Pure): <http://www.rug.nl/research/portal>. For technical reasons the number of authors shown on this cover page is limited to 10 maximum.

Computer Simulation Study of Bipolaron Formation

H. De Raedt

Max-Planck-Institut für Physik und Astrophysik,
Werner-Heisenberg-Institut für Physik, München, Federal Republic of Germany and
Physics Department, University of Antwerp, Wilrijk, Belgium*

A. Lagendijk

Natuurkundig Laboratorium, University of Amsterdam, The Netherlands

Received June 2, 1986

Monte Carlo computer simulation techniques are used to study the formation of bipolarons on a lattice. The transition between the three possible states, extended, two-polaron, and bipolaron is studied. The phase diagram as a function of the strengths of the electron-phonon coupling and repulsive interaction is determined.

I. Introduction

The notion of a polaron, i.e. an electron trapped by the lattice distortion it creates, is relevant for the explanation of wide range of phenomena, found in condensed-matter physics [1]. The ultimate goal of studying polarons is undoubtedly the complete understanding of the many-polaron system. A first and important step towards this ambitious goal is the investigation of bipolaron formation. The creation of bipolarons is in itself an interesting problem as in many theoretical explanations of experiments, the notion of bipolarons is invoked [2-13]. Using a generalization of the method introduced by Emin and Holstein in their study of polaron formation in the adiabatic limit in continuum space, the creation of small-bipolarons has been investigated by Cohen, Economou, and Soukoulis [14]. Another recent study of bipolaron formation has been performed by Hiromoto and Toyozawa [15]. In the latter case the variational approach of Feynman has been extended to include the bipolaron states. An interesting aspect of the work of Hiromoto and Toyozawa is the inclusion of non-adiabaticity. The dynamical properties of bipolarons have been examined by Alexandrov and Ranninger [16], and Kuroda and Mills [17]. In Ref. 14 as well as in Ref. 15, space is

basically treated as a continuum. It has been shown that in polaron models, introduction of a lattice cut-off may seriously influence the outcome [18]. Furthermore results for these continuum-space models are in several case different from those of discrete lattice models [19]. There is no doubt that if in solid-state physics, the lattice version of a model behaves differently compared to the continuous-space version, the lattice equivalent is the most obvious to study.

Computer simulation is probably the most powerful and reliable method known today to study polaron formation on a lattice. Since a polaron is a quantum object, the possibility of large-scale computer simulations of polaron models had to wait for the development of general methods for computer simulation of quantum systems. One of the most versatile ways to perform simulations of quantum systems is through the use of path-integral and path-summation concepts. Interesting in this case is that while these concepts are applicable to many problems they are most ideally suited to study polaron formation. The reason is, of course, that in a path integral formulation it is possible to integrate out the (infinite number of) phonon coordinates analytically, as has been shown by Feynman for the Fröhlich polaron [20].

In this paper we will discuss the formation of bipolarons on a lattice, using computer simulations.

* Permanent address

In our opinion, this “brute-force” numerical experiments are necessary because they provide unbiased information on the model behavior, and there is no need to rely on additional assumptions. As a matter of fact we have to introduce one, and only one approximation which is founded on mathematical theorems concerning exponential operators and is such that all sources of systematic errors due to the approximation are understood and under control. As this is the first computer simulation study of bipolarons on a lattice, it is not wise to examine all possible models and interactions. We have chosen to study a generic three-dimensional model in the adiabatic limit. In addition we have opted for two characteristic and very different forms of the direct electron-electron interaction, viz. a short range and a long range coupling. Our simulations are not restricted to this limit and without any principal difficulty, the method can be extended to include the non-adiabatic regime.

The outline of the paper is as follows. In Sect. 2 we present the theory on which the simulation is based. The inherent quantum mechanical nature of the problem forces us to introduce one (and only) approximation. In Sect. 3 we discuss the simulation technique. We argue that errors on the final results for the relevant physical properties are not determined by the systematic errors resulting from the approximation made, but rather by the limited statistical accuracy that can be achieved by Monte Carlo simulation techniques. The results of our calculations and the conclusions can be found in Sect. 4.

II. Theory

II.1. Model Hamiltonian

The generic Hamiltonian of the lattice model reads

$$H = \sum_{\mathbf{k}, s} \varepsilon(\mathbf{k}) c_{\mathbf{k}, s}^+ c_{\mathbf{k}, s} + \sum_{\mathbf{k}} V(\mathbf{k}) \rho_{\mathbf{k}} \rho_{-\mathbf{k}} + \sum_{\mathbf{k}} Q(\mathbf{k}) (a_{-\mathbf{k}}^+ + a_{\mathbf{k}}) \rho_{\mathbf{k}} + \sum_{\mathbf{k}} \omega(\mathbf{k}) a_{\mathbf{k}}^+ a_{\mathbf{k}}. \quad (2.1)$$

The operators $a_{\mathbf{k}}^+$ ($a_{\mathbf{k}}$) create (annihilate) a phonon excitation of wave vector \mathbf{k} , $c_{\mathbf{k}, s}^+$ ($c_{\mathbf{k}, s}$) create (annihilate) an electron with spin s and $\rho_{\mathbf{k}}$ is the Fourier transformed electron density. In this paper we will, for the sake of simplicity, assume a simple cubic lattice. Hence the electron kinetic energy in (2.1) is given by $\varepsilon(\mathbf{k}) = -2t \sum_{\mu=1}^d \cos k_{\mu}$, where t is the transfer energy associated with nearest-neighbor hopping, $d = 3$ is the dimensionality of the lattice, and

$\mathbf{k} \equiv (k_1, \dots, k_d)$ denotes the wave vector. In general it is difficult to specify the precise form of the electron-electron interaction $V(\mathbf{k})$ since this clearly depends very strongly on the detailed structure of the solid. It is therefore of interest to examine two extremes. We will examine the model for the case of an on-site repulsive interaction between electrons with opposite spins, and as the most common long-range interaction is of the form $1/r$ where r is the distance between the two electrons on the lattice, we will also study this type of interaction with our method. Of course we will have to supplement the latter coupling with an on-site cut-off value. The phonon frequencies $\omega(\mathbf{k})$ and the electron-phonon interactions $Q(\mathbf{k})$ will be specified later on.

In studying bipolaron formation we will, as in recent theoretical studies of this problem [14, 15], assume that it is sufficient to study the properties of model (2.1) for the case where one electron has spin up and the other has spin down. Then the electrons may be considered as being distinguishable. In the following the coordinates of the particles will be denoted by $\mathbf{y}^{(\mu)} \equiv (y_1^{(\mu)}, \dots, y_d^{(\mu)})$, where $\mu = 1, 2$ is the label of a particle.

II.2. Path-Sum Representation

It is well-known that the path-integral formalism is a very powerful tool for calculating properties of continuum polaron models such as the Fröhlich polaron model [20]. Modifying the path-integral expression of the continuum model by introducing a cut-off is not always a safe procedure since it has been shown that the lattice model exhibits some features that be explained by the corresponding continuum model [18, 19], the reason being that in lattice models the kinetic energy is bounded whereas in a continuum model it is not. Although there is no classical Lagrangian for lattice model (2.1) there is no fundamental problem in setting up a path-integral-like framework if the generalized Trotter formula [21] is invoked. Writing H_1 for the electron kinetic energy, H_2 for the electron-electron interaction, and H_3 for the electron-phonon interaction plus free-phonon terms, it follows [21] that the approximant Z_m defined by

$$Z_m = \text{Tr} \left[\exp \left(\frac{-\beta H_1}{m} \right) \exp \left(\frac{-\beta H_2}{m} \right) \exp \left(\frac{-\beta H_3}{m} \right) \right]^m \quad (2.2)$$

will converge to the exact partition function, $Z \equiv \text{Tr} e^{-\beta H} = \lim_{m \rightarrow \infty} Z_m$, and similar results concerning

the convergence can be proven for any expectation value of interest. In practical applications it will, in general, not be possible to take the limit $m \rightarrow \infty$. Keeping m finite is the only approximation that we will make in this work. Of course, it is then necessary to know how the physical properties change with m . Theoretically this problem has been studied extensively and powerful, general theorems on the convergence of approximants such as (2.2) have been proven [21]. In practice, we simply calculate the physical quantities for different values of m and use the general theory [21] to examine the convergence.

To obtain an explicit expression for (2.2) we use the fact that each exponential in (2.2) can be diagonalized separately. Writing each exponent in its diagonal representation, working out the resulting matrix elements and exploiting the fact that, because (2.1) is a quadratic form in the phonon operators, the trace over all phonon coordinates can be carried out analytically, we find that (2.2) can be written as [22]

$$Z_m/Z^P = \sum_{\{y_j^{(\mu)}\}} \prod_{j=1}^m \prod_{\mu=1}^2 \prod_{i=1}^d I \left(\frac{2\beta t}{m}, y_{i,j}^{(\mu)} - y_{i,j+1}^{(\mu)} \right) \cdot \exp \left(-\frac{\beta}{m} V(\mathbf{y}_j^{(1)} - \mathbf{y}_j^{(2)}) \right) \cdot \exp \left(\sum_{j,j'=1}^m \sum_{\mu,\mu'=1}^2 F(j-j', \mathbf{y}_j^{(\mu)} - \mathbf{y}_{j'}^{(\mu')}) \right), \quad (2.3a)$$

where the sum over $\mathbf{y}_j^{(\mu)} \equiv (y_{1,j}^{(\mu)}, \dots, y_{d,j}^{(\mu)})$ runs over all lattice sites, Z^P is the free-phonon partition function and

$$I(z, l) = \frac{1}{L} \sum_{n=1}^L \cos \frac{2\pi ln}{L} \exp \left(z \cos \frac{2\pi n}{L} \right), \quad (2.3b)$$

is the Fourier transform of the imaginary-time lattice propagator of a free particle on a ring of length L . As $I_l(z) = \lim_{L \rightarrow \infty} I(z, l)$, $I(z, l)$ has very similar properties as the modified Bessel functions $I_l(z)$ if $l \ll L$. The effective electron-electron interaction due to the coupling with the phonons is given by

$$F(j, \mathbf{x}) = \frac{\beta^2}{4m^2} \sum_{\mathbf{k}} Q^2(\mathbf{k}) \cdot e^{i\mathbf{k} \cdot \mathbf{x}} \frac{\exp \left(-\frac{j\beta\omega(\mathbf{k})}{m} \right) + \exp \left(-\frac{(m-j)\beta\omega(\mathbf{k})}{m} \right)}{1 - \exp(-\beta\omega(\mathbf{k}))}. \quad (2.3c)$$

For most applications, it is sufficient to consider the model in the adiabatic limit only. This is tantamount to the assumption that the energy scale related to the motion of the electron(s) is much larger than typical phonon energies. Then the elec-

trons adjust instantaneously (on the time scale of the phonon excitations) to the motion of the oscillators. In the present case this implies that in the calculation that lead to (2.3), all contributions of the momentum operators of the phonons should be removed. This changes the trivial prefactor Z^P and the effective interaction $F(j, \mathbf{x})$. Operationally this is equivalent to taking in (2.3c), the limit $\omega(\mathbf{k}) \rightarrow 0$ and (2.3c) simplifies to

$$F(j, \mathbf{x}) = \frac{\beta}{2m^2} \sum_{\mathbf{k}} \frac{Q^2(\mathbf{k})}{\omega(\mathbf{k})} e^{i\mathbf{k} \cdot \mathbf{x}}. \quad (2.4)$$

This is an important result because it shows that the phonon-mediated interaction is determined by a particular combination of $Q(\mathbf{k})$ and $\omega(\mathbf{k})$. In other words, in the adiabatic limit models with different $Q(\mathbf{k})$ and $\omega(\mathbf{k})$ can have the same effective interaction $F(j, \mathbf{x})$. For instance taking dispersionless phonons and an on-site electron-phonon coupling, i.e. taking $Q(\mathbf{k})$ and $\omega(\mathbf{k})$ wave vector independent, or choosing acoustic phonons and a deformation type interaction, i.e. $Q(\mathbf{k}) \sim |\mathbf{k}|^{1/2}$ and $\omega(\mathbf{k}) \sim |\mathbf{k}|$ for small \mathbf{k} , leads to essentially the same effective interaction.

In this paper we will confine ourselves to the case where $Q^2(\mathbf{k})/\omega(\mathbf{k})$ does not depend on \mathbf{k} . Then (2.4) reduces to

$$F(j, \mathbf{x}) = \frac{\beta C}{m^2} \delta_{\mathbf{x}, 0}, \quad (2.5)$$

where C is a collection of constants. It is a nice feature of the assumptions concerning the phonon frequencies and electron-phonon coupling, that in the final expression for Z_m the strength of the electron-phonon interaction is determined by only one parameter C . We still have to specify $V(\mathbf{k})$ or equivalently its Fourier transform $V(\mathbf{x})$ entering (2.3a). As mentioned previously we will study two extremes, namely short-range Coulomb repulsion

$$V(\mathbf{x}) = U \delta_{\mathbf{x}, 0}, \quad (2.6a)$$

and a long-range repulsion

$$V(\mathbf{x}) = \begin{cases} U & \text{if } \mathbf{x} = 0; \\ U/|\mathbf{x}| & \text{otherwise.} \end{cases} \quad (2.6b)$$

From theoretical point of view, introduction of the cut-off in (2.6b) may seem to be somewhat ad hoc but it is quite reasonable if one realizes that for real materials the effective electron-electron potential is obtained by taking into account the atomic (or molecular) wave functions. Our motivation for choosing (2.6b) is to examine the effect of the range of the repulsive interaction on the formation of the bipolaron. The computational technique that we will use

is certainly not restricted to the model potentials (2.6).

II.3. Physical Quantities

The function Z_m/Z^P itself is not of direct interest. More relevant are derivatives of the electron free energy $F_m^E \equiv -(1/\beta) \ln(Z_m/Z^P)$ with respect to the transfer energy t , the electron-phonon coupling C , and the electron-electron potential strength U . To simplify the notation it is convenient to introduce the function

$$\rho(\{\mathbf{y}_j^{(\mu)}\}) \equiv \prod_{j=1}^m \prod_{\mu=1}^2 \prod_{i=1}^d I\left(\frac{2\beta t}{m}, y_{i,j}^{(\mu)} - y_{i,j+1}^{(\mu)}\right) \cdot \exp\left(-\frac{\beta}{m} V(\mathbf{y}_j^{(1)} - \mathbf{y}_j^{(2)})\right) \cdot \exp\left(\sum_{j,j'=1}^m \sum_{\mu,\mu'=1}^2 F(j-j', \mathbf{y}_j^{(\mu)} - \mathbf{y}_{j'}^{(\mu')})\right), \quad (2.7)$$

and to denote the m -th approximant to the expectation value of a quantity A by

$$\langle\langle A \rangle\rangle_m \equiv \frac{\sum_{\{\mathbf{y}_j^{(\mu)}\}} \rho(\{\mathbf{y}_j^{(\mu)}\}) A(\{\mathbf{y}_j^{(\mu)}\})}{\sum_{\{\mathbf{y}_j^{(\mu)}\}} \rho(\{\mathbf{y}_j^{(\mu)}\})}. \quad (2.8)$$

All interesting electron properties can be expressed in terms of these double bracket expectation values. For instance the kinetic energy of the electrons is given by

$$K_m^E \equiv -t \frac{\partial F_m^E}{\partial t} = -\frac{t}{m} \sum_{j=1}^m \sum_{\mu=1}^2 \sum_{i=1}^d \left\langle\left\langle \frac{I\left(\frac{2\beta t}{m}, y_{i,j}^{(\mu)} - y_{i,j+1}^{(\mu)} + 1\right) + I\left(\frac{2\beta t}{m}, y_{i,j}^{(\mu)} - y_{i,j+1}^{(\mu)} - 1\right)}{I\left(\frac{2\beta t}{m}, y_{i,j}^{(\mu)} - y_{i,j+1}^{(\mu)}\right)} \right\rangle\right\rangle_m, \quad (2.9a)$$

and the electron-phonon coupling energy reads

$$V_m^{EP} \equiv -C \frac{\partial F_m^E}{\partial C} = \frac{C}{m^2} \sum_{j,j'=1}^m \sum_{\mu,\mu'=1}^2 \langle\langle \delta_{\mathbf{y}_j^{(\mu)}, \mathbf{y}_{j'}^{(\mu')}} \rangle\rangle_m, \quad (2.9b)$$

and a similar result holds for the potential energy. Since we expect that at least one of these quantities will change rapidly if the system changes from one type of behavior to another one, it is also useful to compute second derivatives of the free energy, i.e. static Kubo susceptibilities. In particular the second derivative of F_m^E with respect to C , i.e. the coupling energy susceptibility,

$$\chi_m^E \equiv -\frac{\partial^2 F_m^E}{\partial C^2} = \frac{\beta}{m^4} \left[\left\langle\left\langle \left(\sum_{j,j'=1}^m \sum_{\mu,\mu'=1}^2 \delta_{\mathbf{y}_j^{(\mu)}, \mathbf{y}_{j'}^{(\mu')}} \right)^2 \right\rangle\right\rangle_m - \left\langle\left\langle \sum_{j,j'=1}^m \sum_{\mu,\mu'=1}^2 \delta_{\mathbf{y}_j^{(\mu)}, \mathbf{y}_{j'}^{(\mu')}} \right\rangle\right\rangle_m^2 \right], \quad (2.10)$$

turns out to be very useful in detecting a transition [22]. When a bipolaron is formed, the distance between the two particles will be less than when no bipolaron is present. Consequently it is worthwhile to investigate the behavior of quantities which are sensitive to a change in relative distance. Following Ref. 15, we will compute

$$D_m \equiv \sqrt{\frac{\left\langle\left\langle \sum_{j=1}^m (\mathbf{y}_j^{(1)} - \mathbf{y}_j^{(2)})^2 \right\rangle\right\rangle_m}{m \langle\langle (\mathbf{y}^{(1)} - \mathbf{y}^{(2)})^2 \rangle\rangle_0}}, \quad (2.11a)$$

where

$$\langle\langle (\mathbf{y}_j^{(1)} - \mathbf{y}_j^{(2)})^2 \rangle\rangle_0 = d \frac{L^2 + 1}{12}, \quad (2.11b)$$

is the mean square relative distance of two free particles moving on a d -dimensional hypercube of linear size L subject to periodic boundary conditions, and serves as a normalization factor.

II.4. Polarons and Bipolarons

Within the context of the path-sum description given above, it is easy to visualize what a polaron or bipolaron state is. Let us first “turn-off” those interactions that will cause the formation of the bipolaron. This means that in the sums over μ and μ' appearing in (2.7-10) we put all contributions with $\mu \neq \mu'$ equal to zero. The resulting path-sum then describes two particles, interacting with their self-generated phonon cloud but not with that of the other, and feeling each other through the potential $V(\mathbf{x})$. If also $V(\mathbf{x})=0$, (2.7) represents two completely independent particles with a self-interaction. In such a system, two independent polarons are formed if C is larger than some value C_{Pol} . Then the self-interaction dominates the kinetic energy and the system changes its state from extended- to polaron-like. In the strong coupling limit, $C \rightarrow \infty$ two polarons are formed and from (2.7) it follows that the configuration of $\mathbf{y}_j^{(\mu)}$ that yields the largest contribution to Z_m/Z^P is $\mathbf{y}_j^{(1)} \equiv \mathbf{y}_j^{(1)}$, $\mathbf{y}_j^{(2)} \equiv \mathbf{y}_j^{(2)}$ for $j=1, \dots, m$. Note that such a configuration does not break translational invariance, as can be certified directly by looking at (2.3a). Using this ansatz we recover the correct binding energy $\lim_{m \rightarrow \infty} F_m^E = -2C$ of the two

polarons. Thus in the path-sum approach, a somewhat crude characterizations of a polaron would be to say that a polaron is formed if $\mathbf{y}_j^{(\mu)} \approx \mathbf{y}_j^{(\mu)}$ for all j , and numerical evidence [19] also demonstrates that this is indeed what happens. It is now easy to conceive what can happen if we turn on the interaction terms with $\mu \neq \mu'$. If we already have two polarons they can either keep their identity or they can form

a bipolaron. In the strong coupling limit a bipolaron state corresponds to $\mathbf{y} = \mathbf{y}_j^{(1)} = \mathbf{y}_j^{(2)}$ for all j . Again such a state is translationally invariant. We have not yet touched upon the role of the Coulomb repulsion which works against the formation of the bipolaron. For the case of the on-site repulsion (2.6a) and in the strong coupling limit it is easy to find out which of the two states, bipolaron or two independent polarons, is realized. Putting $\mathbf{y}^{(1)} = \mathbf{y}_j^{(1)}$ and $\mathbf{y}^{(2)} = \mathbf{y}_j^{(2)}$ for $j = 1, \dots, m$ we obtain

$$\lim_{m \rightarrow \infty} F_m^E = -2C + (U - 2C) \delta_{\mathbf{y}^{(1)}, \mathbf{y}^{(2)}}, \quad (2.12a)$$

so that in this limit the bipolaron state is preferred if

$$U < 2C. \quad (2.12b)$$

To summarize, having an extended state is, in the path-sum representation equivalent to having large deviations of the coordinates $\mathbf{y}_j^{(\mu)}$ from their average value. If the system is in the two-polaron state we expect that $\mathbf{y}^{(\mu)} \approx \mathbf{y}_j^{(\mu)}$ for all j . If a bipolaron is formed we have in addition $\mathbf{y} \approx \mathbf{y}_j^{(\mu)}$ for all j and μ .

III. Numerical Experiments

Calculating numerical values for the physical quantities (2.9-11) for a wide range of values of the parameters C , U , and β (from now on we work in units such that $t=1$) is clearly a non-trivial problem. Disregarding the fact that we are studying a quantum system for a moment, we may interpret (2.8) as the usual expression of an expectation value of a quantity A , the unnormalized density function being given by $\rho(\{\mathbf{y}_j^{(\mu)}\})$. In this sense (2.7) describes a ‘‘classical’’ system of $2m$ particles interacting through nearest-neighbor couplings determined by the functions $I(z, l)$, the potential $V(\mathbf{x})$ and a long-range interaction $F(j, \mathbf{x})$. The quantum mechanical nature of the problem shows up in the strange dependencies of the various couplings on the ‘‘size’’ m of the equivalent classical system.

The proven method that can deal with this complex problem is the Metropolis Monte Carlo technique [23–25]. In the present case, implementation of this technique is not difficult because in contrast to for instance quantum spin systems, no additional fundamental problems related to the quantum nature have to be solved [22]. On the other hand the physics of the problem demands that the model properties are studied at sufficiently low temperature and this imposes some computational constraints. Ideally one would like to know the ground-state properties but if results can only be obtained via simulation this is definitely out of reach. Remember

that the Trotter-Suzuki formula (2.2), upon which the present study is based, requires that one takes the limit $m \rightarrow \infty$ first before one lets $\beta \rightarrow \infty$. As the computation time is of the order m^2 (essentially the time required to move each particle multiplied by the time to compute the change in the self-interaction energy) for large m , it is clear that in practical applications there is a limit, both to m and β .

Comparison with perturbation calculations and experience with similar calculations for the polaron model [19] suggest that $\beta=5$ is sufficiently low temperature, as far as the properties related to the extended-polaron, extended-bipolaron and polaron-bipolaron transition are concerned. To determine the minimum value of m necessary for bringing the systematic error due to the Trotter-Suzuki formula down to an acceptable level, the relevant quantities are computed for several values of m and the convergence as a function of m is examined. For sufficiently large m , the systematic errors disappear in the statistical noise which is always present in Monte Carlo simulations and it then makes no sense to increase m further. The data shown in this paper are obtained from calculations with $m=64, 100$. After making these lengthy calculations it is worthwhile to consider the question whether it is possible to get most of the relevant information with much shorter simulation runs. Of course we do not mean that one should reduce the number Monte Carlo steps per degree of freedom or the number of measurements (11,000, resp. 10,000 for all data presented in this paper) but are referring to performing simulations for smaller m . Indeed it turns out that in order to construct the phase diagram with good confidence it is sufficient to take $m=32$.

The Metropolis Monte Carlo algorithm [23–25] consists of changing the $2m$ degrees of freedom $\mathbf{y}_j^{(\mu)}$ and calculating the corresponding change in $\rho(\{\mathbf{y}_j^{(\mu)}\})$. We use two different schemes to moves through the phase space $\{\mathbf{y}_{k,j}^{(\mu)}\}$. The simplest one is of the most local type: the triple (μ, k, j) is generated randomly and the new coordinate is obtained by adding $+1$ or -1 to $y_{k,j}^{(\mu)}$ each with probability $1/2$. Such a move corresponds to flipping one spin in the Ising spin model [25]. In principle, moves of this type are sufficient in order to reach any point in phase space starting from any other. Thus the Markov chain of states produced by the Metropolis Monte Carlo algorithm is irreducible (also called ‘‘ergodic’’) with a unique limit distribution specified by $\rho(\{\mathbf{y}_j^{(\mu)}\})$ [24]. For obvious practical reasons it is necessary that the important region of phase space is covered in a sufficiently short time. To speed-up relaxation to the equilibrium state a second type of move has been added which makes more global steps through phase space: a pair (μ, k) is selected

randomly and the new trial coordinate is given by $y_{k,j}^{(\mu)} \pm 1$, $j=1, \dots, m$ the + sign being chosen with probability 1/2. In Ising-spin language, such moves would correspond to a multi-spin flip procedure with conservation of total magnetization. Not incorporating this class a moves would make the observation of a polaron-bipolaron transition unlikely if the lattice is large and computer time is limited. We want to emphasize that having this second type of move build into the simulation algorithm is a trick to reduce the computer time required to obtain reliable results, and does not change the physical properties of the system that is being simulated. All simulations reported in this paper have been done with cubes of linear size $L=32$ which for our purposes is large enough because the linear size L only enters our formalism via Z^P and the function $I(z, l)$ (see (2.3b)). In our case $z = 2\beta t/m$ is small and from the properties of $I(z, l)$ (or $I_l(z)$) it then follows that L does not play an important role in determining the physical properties of the system.

To close this section we give some information about the computational resources used in this work. All computations have been done on a CRAY 1S or 2 pipe-line CYBER 205. Because of the non-local interactions, each Monte Carlo step requires a lot of arithmetic operations if m is large enough ($m \leq 100$ for the data presented in this paper). This makes it worthwhile to vectorize the code. For a $m=100$ system, a speedup factor of 7 (12) in CPU-time on the CRAY 1S (CYBER 205) has been obtained by vectorization. Typically, a simulation of a $m=100$ system with 11,000 steps per degree of freedom and 10,000 samples takes about 25 (14) min on a CRAY 1S (CYBER 205).

IV. Simulation Results

As discussed previously, simulation of two completely independent particles interacting with the phonons requires that all contributions with $\mu \neq \mu'$ in the sums over μ and μ' appearing in (2.7-10) are set equal to zero, and this special case is easily incorporated in the simulation program. This is a good test because in this case one is simulating simultaneously two independent systems, each system describing one electron coupled to the lattice, and the results of extensive calculations for these polaron systems have been reported elsewhere [19]. The new simulation program reproduces the results of previous simulations within the statistical errors.

Simulation results for the special case discussed above, obtained by using the newly developed simu-

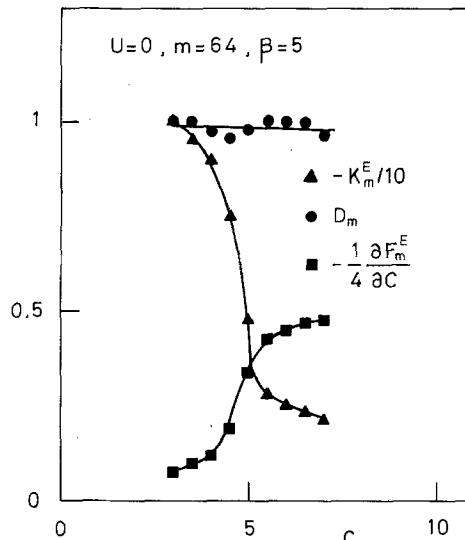


Fig. 1. Monte Carlo results for the kinetic energy (triangles), the distance between the two electrons (dots), and the coupling energy (squares) as a function of the electron-phonon coupling C for the case where all interactions between the two electrons have been turned off. Lines are guide to the eyes only

lation program, are shown in Fig. 1. For $4.5 < C < 5$ the kinetic energy and the coupling energy change rapidly but smoothly. Since all interactions, direct as well as indirect, between the two particles have been turned off the normalized RMS distance D_m fluctuates around 1. Remark that $\partial F_m^E / \partial C$ approaches 2 if C increases, which according to the primitive picture of a polaron sketched in Sect. 2.4 is what we expect to happen. The coupling-energy susceptibility χ_m^E (not shown, see Ref. 22 for examples) exhibits a pronounced peak at $C \approx 4.5$. Exact $T=0$ results for the two-site problem show that χ_m^E is discontinuous as a function of C [26]. A variational calculation, reproducing the exact two-site results and being in excellent agreement with simulation data, has shown that the number of sites, as well as the dimensionality of the lattice is not important as far as the qualitative features of the extended-polaron transition are concerned [19]. Therefore we believe it is justified to interpret a sharp peak in χ_m^E as a signal for a transition from one state to another. Of course, the question whether or not there is a continuous transition cannot be answered by means of simulation. To summarize, Fig. 1 suggests that two independent polarons are formed if $C > C_{\text{Pol}}$ where $C_{\text{Pol}} \approx 4.5$.

If the electron-phonon mediated interaction between the electrons is switched on, the same quantities as those shown in Fig. 1 behave differently, as demonstrated in Fig. 2. First we note that the RMS distance D_m jumps from its free-particle value 1 to almost zero if $C > C_{\text{Bip}}$. This already signals the

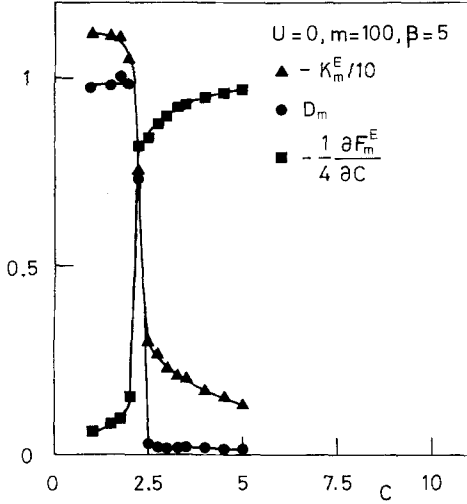


Fig. 2. Monte Carlo results for the kinetic energy (triangles), the distance between the electrons (dots), and the coupling energy (squares) as a function of the electron-phonon coupling C for the case where the repulsive interaction between the two electrons is zero. A bipolaron is formed if $C > 2.5$. Lines are guide to the eyes only

formation of a bipolaron. From Fig. 2 we estimate that $C_{\text{Bip}} \approx 2.5$. Additional confirmation regarding the formation of a bipolaron can be obtained by noting that for a bipolaron state, one expects that for increasing C , $\partial F_m^E / \partial C$ approaches 4 and, as shown in Fig. 2, this is indeed the case. On a more qualitative level we observe that the transition from extended to bipolaron state is much more abrupt than the extended-polaron transition, as can for instance be seen by comparing slopes of the kinetic energy K_m^E in the transition regime.

Up to now the repulsive interaction between the particles has not been included. As explained above, one expects that by increasing the strength of the repulsive interaction, it should be possible for the system to form, in addition to the extended- or bipolaron state already observed, a two-polaron state, depending on the strength of the electron-phonon coupling C . For a long range potential of the type (2.6b) and $U = 50$ the simulation results are given in Fig. 3. The value of U was chosen such that the three different situations, extended, two-polaron, and bipolaron are clearly visible. The value of $C_{\text{Pol}} \approx 4.5$ does not change with U , at least not within the statistical accuracy. In the regime $C_{\text{Pol}} < C < 6$ all quantities change smoothly. For $6 < C < 7$ the coupling energy and D_m change drastically. If $C > 7$, $\partial F_m^E / \partial C$ has reached its strong coupling value 4 and D_m is essentially zero. From Fig. 3 we estimate that $C_{\text{Bip}} \approx 6.7$ if $U = 50$. By repeating the analysis for different U , it is straightforward to map out the phase diagram. The $U-C$ phase diagram for the

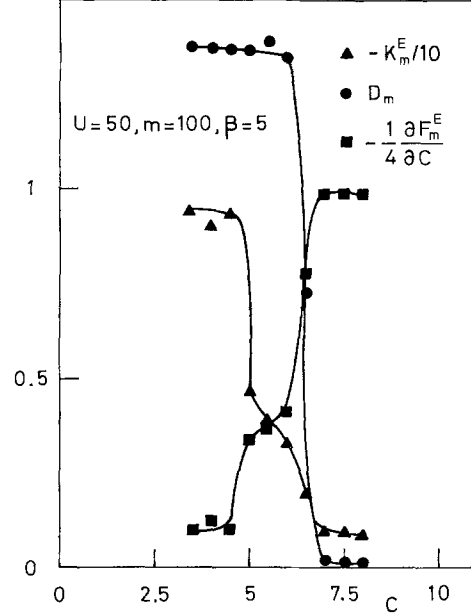


Fig. 3. Simulation results for the kinetic energy (triangles), the distance between the electrons (dots), and the coupling energy (squares) as a function of the electron-phonon coupling C for a long-range interaction of the form (2.6b) and $U = 50$. The transition from extended to polaron state occurs at $C \approx 4.7$, the bipolaron is formed if $C > 6.5$. Lines are guide to the eyes only

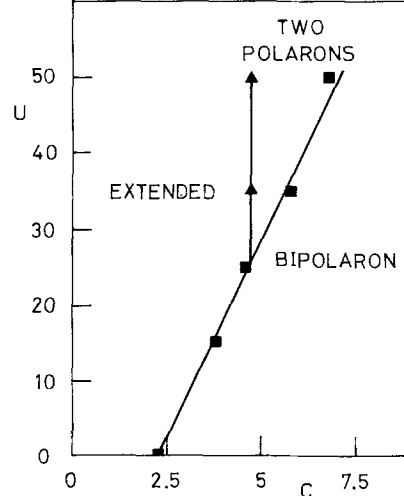


Fig. 4. $U-C$ phase diagram for a long-range interaction of the form (2.6b) and $U = 50$. Lines are guide to the eyes only

case of the long-range potential (2.6b) is depicted in Fig. 4. Within the accuracy of the simulations, the separatrix between extended and two-polaron regime is vertical. This is to be expected since in both regimes there is no polaron-polaron correlation. We want to emphasize that the extended - two-polaron transition is a smooth one [19], certainly not as abrupt as the transition to a bipolaron state.

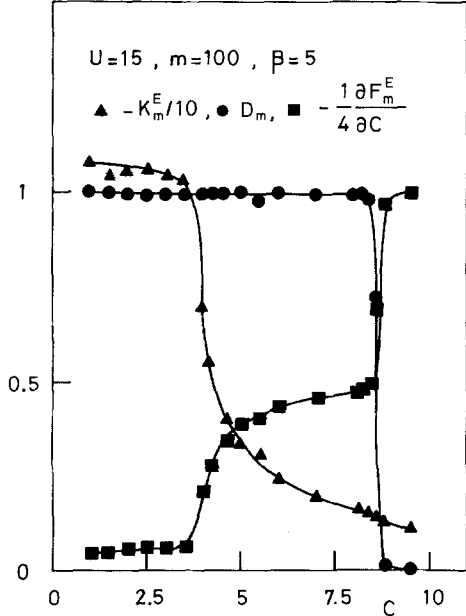


Fig. 5. Simulation results for the kinetic energy (triangles), the distance between the electrons (dots), and the coupling energy (squares) as a function of the electron-phonon coupling C for an on-site Coulomb repulsion $U=15$. The transition from extended to polaron state occurs at $C \approx 4.5$, the bipolaron is formed if $C > 8.5$. Lines are guide to the eyes only

Exactly the same procedure as the one outline above has been followed to analyze the simulation data for the case of the on-site repulsive interaction (2.6a). Qualitatively, the results are very similar and therefore it is not necessary to display all results. The simulation results for the same quantities as those depicted in Figs. 1, 3, as obtained from simulations with an on-site repulsive interaction of strength $U=15$, are shown in Fig. 5. It is clear that as the coupling strength C increases, the system undergoes two successive transitions. In Fig. 6, data for the coupling-energy susceptibility χ_m^E for $U=15$ is given (for the long-range potential, the corresponding plot looks similar). The maximum at $C \approx 4.5$ signals the transition from extended to two-polaron state. The value of C at which the maximum occurs (C_{P0}), is the same as the value determined by single polaron simulations [19]. As the coupling to the phonons is the driving field for the formation of both the polaron(s) and the bipolaron, and χ_m^E is the corresponding fluctuation of this interaction energy, one expects to see a second maximum in χ_m^E if a bipolaron is formed. As shown by Fig. 6, this second peak is indeed observed. This gives supports to our believe that χ_m^E is indeed a convenient quantity for detecting transitions of this kind.

Applying the same analysis as the one used above to the data of the other physical quantities it

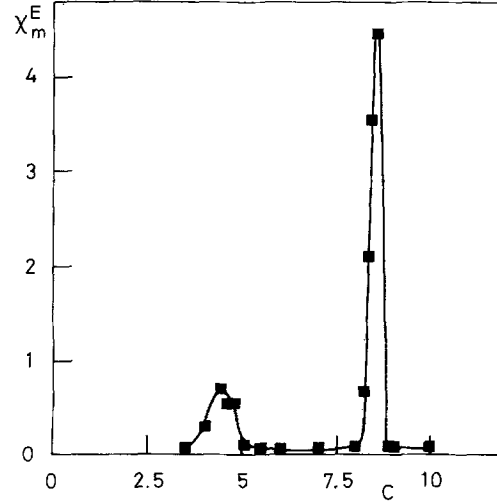


Fig. 6. Simulation results for the electron-phonon coupling energy susceptibility as a function of C for an on-site Coulomb repulsion $U=15$. The peak at $C \approx 4.5$ signals the formation of two polarons, the peak at $C \approx 8.5$ indicates the formation of the bipolaron. For a qualitative picture of the behavior of other quantities see Figs. 2, 3. Lines are guide to the eyes only.

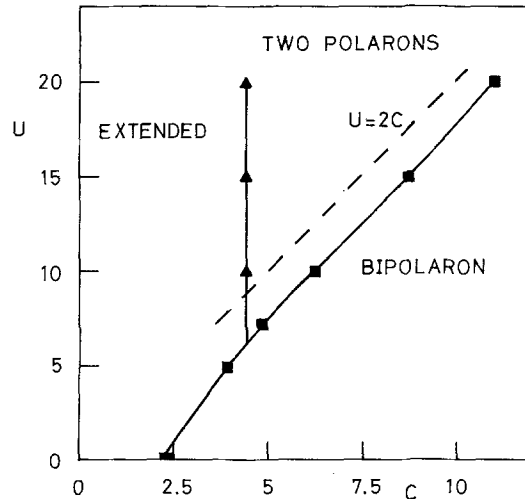


Fig. 7. $U-C$ phase diagram for an on-site Coulomb interaction. The dashed line is the prediction of simple strong-coupling theory for the two-polarons-bipolaron transition. Solid lines are guide to the eyes only

follows unambiguously that the bipolaron is formed if $C > C_{\text{Bip}} \approx 8.5$ (for the case $U=15$). The complete $U-C$ phase diagram is shown in Fig. 7. The slope of the two-polaron-bipolaron separatrix is approximately equal to 2, in good agreement with the elementary theoretical argument given in Sect. 2.4 (see 2.12b) but the estimate for the critical coupling for bipolaron formation C_{Bip} is wrong by about 10%.

As pointed out in Ref. 15, it is of interest to compare the unnormalized RMS distance with the

lattice spacing (which was taken to be 1 throughout this work). When the bipolaron is formed, our results for the unnormalized RMS distance are always much less than the lattice spacing, indicating that in this state the two particles are almost always on the same site. This situation is changed when formation of the bipolaron is due to an electron-phonon interaction of the Fröhlich type [15]. Although some aspects of polaron formation depend whether or not the continuum limit of the lattice model is considered [18, 19], for the three dimensional lattice model studied in this paper, the general features of the phase diagrams are quite similar.

We would like to thank W. Götzte for stimulating discussions and useful suggestions. This work is partially supported by the "Supercomputer Project" of the National Science Foundation, Belgium. One of us (H.D.R) thanks the National Science Foundation, Belgium for financial support.

References

1. Mahan, G.D.: Many particle physics. New York: Plenum Press 1981
2. Anderson, P.W.: Phys. Rev. Lett. **34**, 953 (1975)
3. Street, R.A., Mott, N.F.: Phys. Rev. Lett. **35**, 1293 (1975)
4. Kastner, M., Adler, D., Frzitsche, H.: Phys Rev. Lett. **37**, 1504 (1976)
5. Chakraverty, B.K., Sienko, M.J.: Phys. Rev. B **17**, 3781 (1978)
6. Baraff, G.A., Kane, E.O., Schlüter, M.: Phys. Rev. Lett. **43**, 956 (1979)
7. Schirmer, O.F., Salje, E.: J. Phys. C **13**, L1067 (1980)
8. Watkins, G.D., Troxel, J.R.: Phys. Rev. Lett. **44**, 593 (1980)
9. Onoda, M., Nagasawa, H.: Solid State Commun. **39**, 1125 (1981)
10. Takahashi, T., Nagasawa, H.: Solid State Commun. **39**, 1125 (1981)
11. Onoda, M., Takahashi, T., Nagasawa, H.: J. Phys. Soc. Jpn. **51**, 3868 (1982)
12. Cade, N.A., Movaghar, B.: J. Phys. C **16**, 539 (1983)
13. Chance, R.R., Brédas, J.L., Silbey, R.: Phys. Rev. B **29**, 4491 (1984)
14. Cohen, M.H., Economou, E.N., Soukoulis, C.M.: Phys. Rev. B **29**, 4496 (1985)
15. Hiramoto, H., Toyozawa, Y.: J. Phys. Soc. Jpn. **54**, 245 (1985)
16. Alexandrov, A., Ranninger, J.: Phys. Rev. B **23**, 1796 (1981)
17. Kuroda, Y., Mills, D.L.: Phys. Rev. B **31**, 7624 (1985)
18. Das Sarma, S.: Solid State Commun. **54**, 1067 (1985)
19. Lagendijk, A., De Raedt, H.: Phys. Lett. **108A**, 91, (1985)
20. Feynman, R.P., Hibbs, A.R.: Quantum mechanics and path integrals. New York: McGraw-Hill 1965
21. Suzuki, M.: Prog. Theor. Phys. **56**, 1454 (1976)
Suzuki, M.: J. Math. Phys. **26**, 601 (1985)
Suzuki, M.: Phys. Rev. B **31**, 2957 (1985)
22. De Raedt, H., Lagendijk, A.: Phys. Rep. **127**, 233 (1985)
23. Metropolis, N., Rosenbluth, A.W., Rosenbluth, M.N., Teller, A.H., Teller, E.: J. Chem. Phys. **21**, 1087 (1953)
24. Hammersley, J.M., Handscomb, D.C.: Monte Carlo methods. London: Methuen 1964
25. Binder, K., Stauffer, D.: Application of the Monte Carlo method. In statistical physics. In: Topics in Current Physics. Vol. 36, Binder, K. (ed.). Berlin, Heidelberg, New York: Springer 1984
26. De Raedt, B., De Raedt, H.: Phys. Rev. B **29**, 5325 (1983)

H. De Raedt
Max-Planck-Institut
für Physik und Astrophysik
Werner-Heisenberg-Institut für Physik
Postfach 401212
D-8000 München
Federal Republic of Germany

and

Physics Department
University of Antwerp
Universiteitsplein 1
B-2610 Antwerpen (Wilrijk)
Belgium

A. Lagendijk
Natuurkundig Laboratorium
University of Amsterdam
Valckenierstraat 65
NL-1018 XE Amsterdam
The Netherlands